

## Granular magnetoresistance in cobalt/poly (3-hexylthiophene, 2, 5-diyl) hybrid thin films prepared by a wet chemical method

Tianlong Wen, Dan Liu, Christine K. Luscombe, and Kannan M. Krishnan<sup>a)</sup>

*Department of Materials Science and Engineering, University of Washington, Box 352120, Seattle, Washington 98195-2120, USA*

(Received 1 June 2009; accepted 8 August 2009; published online 27 August 2009)

Cobalt/poly (3-hexylthiophene, 2, 5-diyl) (P3HT) hybrid thin films were prepared by a wet chemical method. Their microstructure consists of a nanoscale mixture of a crystalline P3HT matrix, interspersed with amorphous P3HT regions containing the cobalt nanoparticles. Magnetic and transport measurements are consistent with this microstructure and the temperature dependence of the resistance of these hybrid systems is well-fitted ( $R^2=0.9993$ ) to the fluctuation induced tunneling model. Moreover, by applying a magnetic field, a magnetoresistance ratio of 3% was observed in 17 vol % Co hybrid films at 10 K. © 2009 American Institute of Physics. [DOI: 10.1063/1.3213561]

The interplay between electrical transport and an applied magnetic field in various inorganic, ferromagnetic materials systems, and morphologies, as demonstrated by the observations of anisotropic magnetoresistance,<sup>1</sup> tunneling magnetoresistance (TMR),<sup>2</sup> and giant magnetoresistance,<sup>3</sup> is now well-established. These phenomena have significant meaning both in understanding the fundamental physical principles of spin transport<sup>4</sup> and in practical applications.<sup>5</sup> Specifically, magnetoresistance can be exhibited in magnetic/nonmagnetic thin film heterostructures<sup>6</sup> as well as in systems where granular magnetic entities are embedded in a nonmagnetic matrix.<sup>7,8</sup>

Complementing the above, spin transport in organic semiconductors has recently emerged as a viable alternative for spintronics<sup>9</sup> largely because of the potentially long spin-relaxation time in organic materials<sup>10</sup> arising from their inherently weak spin-orbit coupling. This is also consistent with the current trend of employing organic semiconducting materials in various electronic devices including solar cells,<sup>11</sup> diodes,<sup>12</sup> transistors,<sup>13</sup> and flexible displays<sup>14,15</sup> with potential advantages that include flexibility of the material system, ease of processability, and the potential to make light-weight and low-cost devices.<sup>9</sup> However, the development of an all-organic, physically flexible, magnetoresistance device is currently not possible because, to the best of our knowledge, no suitable ferromagnetic organic material has been found so far. Nevertheless, preliminary TMR (Ref. 16) results using an organic semiconducting (OSC) material, i.e., tris(8-hydroxyquinolino) aluminum ( $\text{Alq}_3$ ), as a nonmagnetic spacer in a ferromagnet/OSC/ferromagnet sandwich structure, are promising. In this context, we report magnetoresistance measurements in a hybrid system comprised of cobalt magnetic nanoparticles (Co MNPs) embedded in a semiconducting poly(3-hexylthiophene, 2,5-diyl) (P3HT) polymer matrix. Since the semiconducting polymer matrix is flexible, this composite device can potentially be a good candidate for a structurally flexible magnetoresistance device. Unlike other magnetoresistance devices that were prepared by physical methods and require extreme conditions, these composite devices were prepared by a wet-chemical method, which can largely reduce the cost and simplify the processing. Further-

more, because cobalt nanoparticles passivated with organic surfactant can be mixed uniformly with P3HT with any ratio in an organic solvent, composite films with different cobalt concentration can be easily obtained. Finally, we contribute to the ongoing debate on the underlying mechanism of spin transport in organic materials and demonstrate a good fit of the temperature-dependent resistivity data to a fluctuation induced tunneling (FIT) model for our sample.

Cobalt nanoparticles were synthesized by the well-established thermal decomposition procedure by injecting cobalt carbonyl [ $\text{Co}_2(\text{CO})_8$ ] into a hot solution of 1,2-dichlorobenzene in the presence of surfactant.<sup>17</sup> The as-synthesized cobalt nanoparticles, coated with oleic acid as stabilizer to prevent the particle from aggregating and oxidizing, are then washed, precipitated with ethanol, and dried. Then 6 mg P3HT and various amount of dried cobalt was codissolved by sonicating in 600  $\mu\text{l}$  toluene, and stirred for 4 h at 45 °C to make P3HT/Co nanoparticles solutions with different ratios. Films were made by drop casting 63  $\mu\text{l}$  of the mixed solution onto an indium tin oxide glass substrate to yield a Co/P3HT hybrid film. The film was annealed in 5 vol %  $\text{H}_2$ /95 vol % Ar atmosphere for 2 h at 150 °C, and then a gold contact strip was deposited on top of the film by evaporation to perform transport measurements in a quantum design physical property measurement system (PPMS). Slices of the composite films were made by microtome and put on Cu grids and their microstructure characterized by scanning transmission electron microscopy (STEM) using a FEI Tecnai G2 F20 microscope operating at 200 kV. The crystalline structure of the composite film, the pure P3HT film and cobalt nanoparticle powders were characterized by  $\theta$ -2 $\theta$  x-ray diffraction (XRD) with the Cu  $K\alpha$  radiation ( $\lambda=1.54$  Å).

P3HT is a well-known semiconducting ( $\sigma\sim 10^{-6}$ – $10^{-7}$  S/cm for pressed pellet,<sup>18</sup> and  $\sigma\sim 10^{-8}$ – $10^{-9}$  S/cm for cast film<sup>19</sup>) and semicrystalline<sup>20,21</sup> (a mixture of crystalline lamella and amorphous domains on the nanometer length scale) polymer widely used in organic electronics.<sup>22</sup> Further, the hexyl group on the polymer chain of P3HT makes it possible to process it easily in an organic solvent environment.<sup>22</sup> In addition, because the cobalt nanoparticles are stabilized by a layer of surfactant with a hydrophobic tail, it is possible to completely codisperse P3HT and cobalt

<sup>a)</sup>Electronic mail: kannanmk@u.washington.edu.

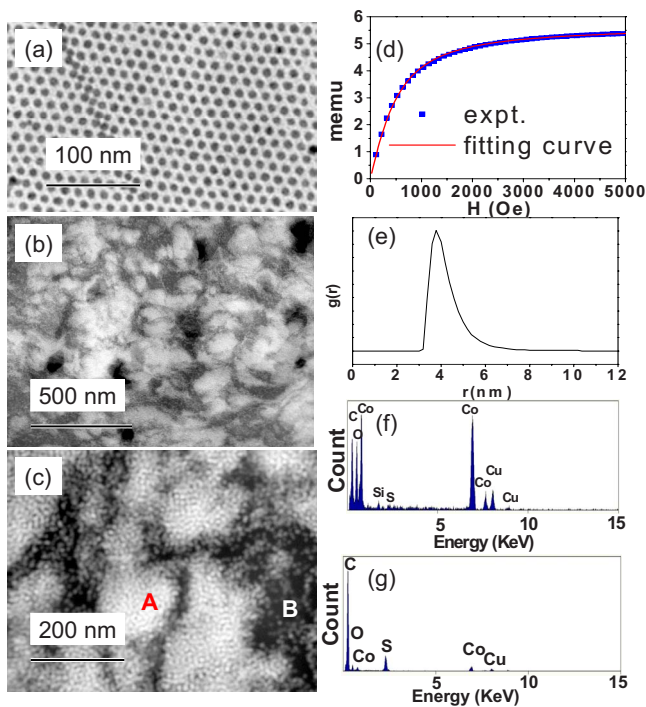


FIG. 1. (Color online) (a) TEM image of as-synthesized Co MNPs; [(b) and (c)] the STEM image of Co/P3HT hybrid film (15 vol % Co) (d) Chantrell's fitting with experiment data of the composite film, the fitting gives the magnetic diameter of 7.6 nm with standard deviation of 0.6 nm; (e) the size distribution extracted from Chantrell's fitting (Ref. 24) by assuming log-normal distribution; and [(f) and (g)] representative EDX spectra collected at points A and B in (c), respectively.

nanoparticles in an organic solvent, and make a composite film with any ratio of cobalt and P3HT. The physical diameter,  $d_o$ , of the cobalt nanoparticles, determined by TEM observation of the as-synthesized cobalt nanoparticles [Fig. 1(a)] is  $d_o \sim 8$  nm, which is within the regime of superparamagnetism.<sup>23</sup> Figures 1(b) and 1(c) shows the dark field image of the hybrid film obtained by STEM observation. Due to the atomic-number or  $Z$ -contrast, aggregates of cobalt nanoparticles (bright areas), separated by the dark areas of P3HT can be clearly resolved. The magnetic size,  $d_m$ , of the cobalt nanoparticles in the hybrid film were measured by fitting the  $M$ - $H$  curve of the composite film with Chantrell's method [Fig. 1(d)],<sup>24</sup> assuming a log normal size distribution of the cobalt nanoparticles, giving  $d_m \sim 7.6$  nm with standard deviation of 0.6 nm [Fig. 1(e)]. The x-ray diffraction of the composite film with different concentrations of cobalt is shown in Fig. 2. The peak at  $44.2^\circ$  corresponds to the (221) crystallographic planes of  $\epsilon$ -Co;<sup>25</sup> and the peaks at  $5.4^\circ$ ,  $10.8^\circ$ , and  $16^\circ$  correspond to (100), (200), and (300)  $a$ -axis diffraction peaks of P3HT.<sup>26</sup> The peak intensity of P3HT at  $2\theta=5.4^\circ$ , observed to be inversely related to the concentration of cobalt nanoparticles in the hybrid films, is proportional either to the number of the nanodomains of crystalline P3HT per unit volume<sup>26</sup> or to the number of domains with  $a$ -axis oriented normal to the substrate surface.<sup>21</sup> The films cast from solution prefer an alignment with  $a$ -axis normal to the substrate<sup>21</sup> and this does not change with the addition of cobalt nanoparticles into the films since no peak at  $2\theta=23^\circ$  corresponding to the  $b$ -axis and  $c$ -axis is observed.<sup>26</sup> Hence, we conclude that the addition of cobalt nanoparticles results in the unfolding of some P3HT crystalline lamella nanodomains rendering them amorphous. More-

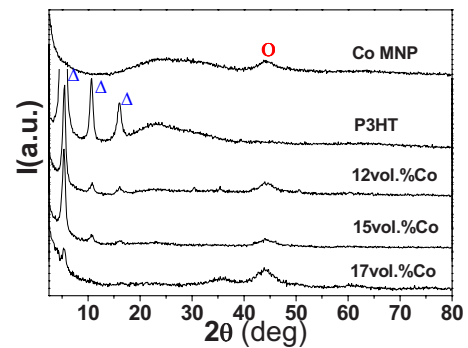


FIG. 2. (Color online) X-ray  $\theta$ - $2\theta$  diffraction scans of Co MNPs, P3HT, and their composite film. Peaks ( $\Delta$ ) at  $5.4^\circ$ ,  $10.8^\circ$ , and  $16^\circ$  correspond to (100), (200), and (300)  $a$ -axis orientations of P3HT; and the peak ( $\circ$ ) at  $44.2^\circ$  corresponds to the (221) crystallographic planes of  $\epsilon$ -Co.

over, combined with our STEM observations, we can infer that the cobalt nanoparticles are distributed in the amorphous region of P3HT polymers. Further, addition of cobalt nanoparticles into the P3HT matrix unfold some P3HT crystalline lamella nanodomains to accommodate these cobalt nanoparticles<sup>27</sup> so that as many crystalline regions of the P3HT as possible can be preserved to minimize the free energy of the whole system. This in turn will reduce the number of the crystalline nanodomains of the P3HT per unit volume, and thus reduce the intensity of the  $\theta$ - $2\theta$  XRD peak at  $5.4^\circ$ .

To investigate the conduction mechanism in the P3HT polymer as well as in the hybrid system, temperature dependent resistance,  $\rho(T)$ , of both films were measured by a standard four-terminal technique in the PPMS system. Pure P3HT with the same concentration has a resistance beyond the measurement limit of the PPMS system. Thus we can say that the conduction observed for the hybrid film is via electron tunneling between the highly conducting regions containing cobalt nanoparticles distributed in the amorphous regions of the P3HT. Moreover,  $\rho(T)$  of the hybrid system is best-fitted ( $R^2=0.9993$ ) to the fluctuation induced tunneling (FIT) model,<sup>28,29</sup> used to describe charge transport in carbon-poly(vinyl chloride) systems, i.e.,  $\rho(T)=\rho_o \exp[T_1/(T+T_o)]$  at low temperature, where  $k_B T_1$  is the energy required for an electron to tunnel across the polymer gap between conducting particle aggregates and for  $T \ll T_o$  the resistivity is temperature-independent.<sup>28</sup> In this FIT model, the highly conducting regions containing small particle aggregates are separated by a less conducting polymer matrix, which is analogous to the observed microstructure in these hybrid samples. The temperature-dependence of the resistivity of the 12 vol % Co hybrid film without applied magnetic field [Fig. 3(a)], shows good agreement with the FIT model below 100 K. The upturn in resistivity at low temperatures, were also fitted to a number of other mechanisms, from localization ( $\rho \sim T^{-p/2}$ ,  $\rho \sim \ln T$ ,  $\rho \sim T^{p/2}$ , in different dimensions)<sup>29</sup> to variable range hopping [ $\ln(\rho) \sim T^{-1/(1+d)}$ ],<sup>28</sup> but all these fittings were inferior (only fits to VRH is also shown in Fig. 3) to the FIT model. Finally, the increase in resistance with temperature above 100 K is consistent with the interpretation<sup>28</sup> that the energy barrier between cobalt aggregates will be reduced by thermal fluctuation, but will be widened by the rapid physical expansion of the polymer as temperature increase; the competition between these two effects will result in a minimum resistance<sup>28</sup> and the barrier for tun-

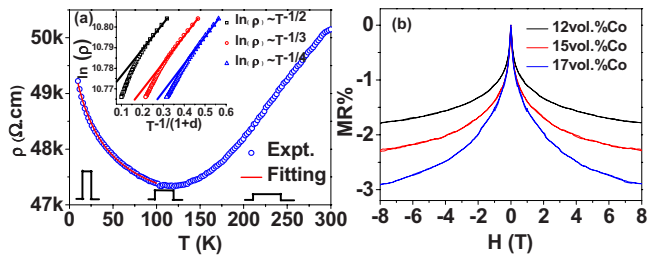


FIG. 3. (Color online) (a) The dependence of resistance of the 12 vol % Co hybrid film on temperature is well-fitted to the fluctuation-induced tunneling (FIT) conduction model (adjusted  $R^2=0.9993$ ) at low temperature (nonlinear curve fitting using ORIGIN software), giving  $T_1=2.2$  K and  $T_0=31$  K. The turning point is due to the differential thermal expansion between cobalt and P3HT matrix.  $\ln(\rho) \sim T^{-1/(1+d)}$  curves ( $d=1, 2,$  and  $3$ ) for variable range hopping at  $T < 100$  K are also plotted (inset) and these curves are a poor fit with significant deviation from the expected straight line. (b) The resistance change at 10 K of Co/P3HT hybrid composite film, for different nanoparticle concentrations, as a function of the externally applied magnetic field.

neling at different temperatures is as depicted in the inset of Fig. 3(a).

The magnetoresistance of several Co/P3HT hybrid composite films with different composition, and up to an applied field of 8 Tesla, was measured for the temperature range from 10 to 300 K. Figure 3(b) shows magnetoresistance ratio of Co/P3HT hybrid composite film of three different compositions with respect to applied magnetic field at 10 K, in which the magnetoresistance is defined as  $MR\% = [\rho(H) - \rho(0)]/\rho(0)$ , where  $\rho(H)$  and  $\rho(0)$  are resistivity of the composite film at the applied field of  $H$  and 0, respectively. As shown in Fig. 3(b), the resistivity of the composite film decreases as the external magnetic field increases, and continues to decrease slowly even at an external magnetic field of 8 Tesla. Meanwhile, if the concentration of the cobalt magnetic nanoparticles increases from 12 vol % Co to 17 vol % Co, the magnetoresistance ratio of the hybrid composite film at 8 T increase from 1.8% to 2.9%. As the temperature increases, the magnetoresistance ratio of these hybrid films decreases rapidly, which is trivial at 200 K and disappears at room temperature. As discussed above, the conduction of electron in these hybrid composite films is via the tunneling between the highly conducting region containing cobalt nanoparticles in the P3HT amorphous region through the crystalline region of P3HT. Thus we propose that when electrons tunnel between these conduction regions, the tunneling probability for the spin-up and spin-down electrons is different and leads to different resistances when the magnetization configuration of these nanoparticles are altered from random to being parallel to the applied magnetic field.<sup>30</sup>

In conclusion, Co/P3HT composite films were prepared by a wet chemical method for the purpose of electron transport investigation. The electron transport in this hybrid system is via tunneling between regions containing cobalt nanoparticles aggregate in the composite film. A magnetoresistance ratio of 3% was observed for the 17 vol % Co sample at 10 K. Compared to ferromagnet/OSC/ferromagnet sandwich structures investigated by many groups,<sup>9,16</sup> the Co/P3HT hybrid system allows us to investigate spin transport in a hybrid organic granular system. In contrast to devices with inorganic/organic sandwich structures, the granular/hybrid system can be made physically flexible, though the

MR ratio is still small and cannot be retained at room temperature. Further enhancement of the device performance can be envisioned by optimizing the material system and the microstructure as well as by improving electrode contact. Such work is in progress.

This project is partially supported by National Science Foundation DMR Grant Nos. 0501421, 0120967, and 0747489 and the Murdock Foundation. Part of this work was conducted at the University of Washington NanoTech User Facility, a member of the NSF National Nanotechnology Infrastructure Network (NNIN).

- <sup>1</sup>T. R. McGuire and R. I. Potter, *IEEE Trans. Magn.* **11**, 1018 (1975).
- <sup>2</sup>J. S. Moodera, L. R. Kinder, T. M. Wong, and R. Meservey, *Phys. Rev. Lett.* **74**, 3273 (1995).
- <sup>3</sup>M. N. Baibich, J. M. Broto, A. Fert, F. N. Vandau, F. Petroff, P. Eitenne, G. Creuzet, A. Friederich, and J. Chazelas, *Phys. Rev. Lett.* **61**, 2472 (1988).
- <sup>4</sup>J. F. Gregg, I. Petej, E. Jouguelet, and C. Dennis, *J. Phys. D: Appl. Phys.* **35**, R121 (2002).
- <sup>5</sup>S. A. Wolf, D. D. Awschalom, R. A. Buhrman, J. M. Daughton, S. V. Molnar, M. L. Roukes, A. Y. Chtchelkanova, and D. M. Treger, *Science* **294**, 1488 (2001).
- <sup>6</sup>R. L. White, *IEEE Trans. Magn.* **28**, 2482 (1992).
- <sup>7</sup>A. E. Berkowitz, J. R. Mitchell, M. J. Carey, A. P. Young, S. Zhang, F. E. Spada, F. T. Parker, A. Hutten, and G. Thomas, *Phys. Rev. Lett.* **68**, 3745 (1992).
- <sup>8</sup>J. Q. Xiao, J. S. Jiang, and C. L. Chien, *Phys. Rev. Lett.* **68**, 3749 (1992).
- <sup>9</sup>W. J. M. Naber, S. Faez, and W. G. van der Wiel, *J. Phys. D: Appl. Phys.* **40**, R205 (2007).
- <sup>10</sup>A. R. Rocha and S. Sanvito, *J. Comput. Theor. Nanosci.* **3**, 624 (2006).
- <sup>11</sup>K. M. Coakley and M. D. McGehee, *Chem. Mater.* **16**, 4533 (2004).
- <sup>12</sup>G. Gustafsson, Y. Cao, G. M. Treacy, F. Klavetter, N. Colaneri, and A. J. Heeger, *Nature (London)* **357**, 477 (1992).
- <sup>13</sup>F. Garnier, R. Hajlaoui, A. Yassar, and P. Srivastava, *Science* **265**, 1684 (1994).
- <sup>14</sup>C. J. Drury, C. M. J. Mutsaers, C. M. Hart, M. Matters, and D. M. de Leeuw, *Appl. Phys. Lett.* **73**, 108 (1998).
- <sup>15</sup>G. H. Gelinck, H. E. Huitema, E. V. Veenendaal, E. Cantatore, L. Schrijnemakers, J. B. P. H. V. D. Putten, T. C. T. Geuns, M. Beenhakkers, J. B. Giesbers, B. H. Huisman, E. J. Meijer, E. M. Benito, F. J. Touwslager, A. W. Marsman, B. J. E. V. Rens, and D. M. Deleeuw, *Nature Mater.* **3**, 106 (2004).
- <sup>16</sup>T. S. Santos, J. S. Lee, P. Migda, I. C. Lekshimi, B. Satpati, and J. S. Moodera, *Phys. Rev. Lett.* **98**, 016601 (2007).
- <sup>17</sup>V. F. Puentes, K. M. Krishnan, and A. P. Alivisatos, *Science* **291**, 2115 (2001).
- <sup>18</sup>T. A. Chen, X. Wu, and R. D. Rieke, *J. Am. Chem. Soc.* **117**, 233 (1995).
- <sup>19</sup>S. A. Chen and C. S. Liao, *Macromolecules* **26**, 2810 (1993).
- <sup>20</sup>S. Malik and A. K. Nandi, *J. Polym. Sci., Part B: Polym. Phys.* **40**, 2073 (2002).
- <sup>21</sup>H. Sirringhaus, P. J. Brown, R. H. Friend, M. M. Nielsen, K. Bechgaard, B. M. W. Langeveld-Voss, A. J. H. Spiering, R. A. J. Janssen, E. W. Meijer, P. Herwig, and D. M. de Leeuw, *Nature (London)* **401**, 685 (1999).
- <sup>22</sup>Z. Bao, A. Dodabalapur, and A. J. Lovinger, *Appl. Phys. Lett.* **69**, 4108 (1996).
- <sup>23</sup>K. M. Krishnan, A. B. Pakhomov, Y. Bao, P. Blomqvist, Y. Chun, M. Gonzales, K. Griffin, X. Ji, and B. K. Roberts, *J. Mater. Sci.* **41**, 793 (2006).
- <sup>24</sup>S.-H. Yoon, M. Gonzales-Weimuller, Y.-C. Lee, and K. M. Krishnan, *J. Appl. Phys.* **105**, 07B507 (2009).
- <sup>25</sup>V. F. Puentes and K. M. Krishnan, *Appl. Phys. Lett.* **78**, 2187 (2001).
- <sup>26</sup>T. Erb, U. Zhokhavets, G. Gobsch, S. Raleva, B. Stühn, P. Schilinsky, C. Waldauf, and C. J. Brabec, *Adv. Funct. Mater.* **15**, 1193 (2005).
- <sup>27</sup>S. Yeh, T. Wu, K. Wei, Y. Sun, and K. Liang, *J. Polym. Sci., Part B: Polym. Phys.* **43**, 1220 (2005).
- <sup>28</sup>E. K. Sichel, J. I. Gittleman, and P. Sheng, *Phys. Rev. B* **18**, 5712 (1978).
- <sup>29</sup>P. A. Lee and T. V. Ramakrishnan, *Rev. Mod. Phys.* **57**, 287 (1985).
- <sup>30</sup>M. Holdenried, B. Hackenbroich, and H. Micklitz, *J. Magn. Magn. Mater.* **231**, 13 (2001).